Journal of Solid State Chemistry 219 (2014) 191–200

Contents lists available at ScienceDirect

Journal of Solid State Chemistry

journal homepage: www.elsevier.com/locate/jssc

Synthesis and characterisation of In-doped $MnWO_4$-type solid-solutions: $Mn_{1-3x}In_{2x}\square_xWO_4$ ($x=0$–0.11)

U. Gattermann [a], S.-H. Park [a,*], M. Kaliwoda [b]

[a] Section Crystallography, Department for Earth and Environmental Sciences, Ludwig-Maximilians-Universität München, Theresienstrasse 41, 80333 Munich, Germany

[b] Mineralogische Staatssammlung München, Theresienstrasse 41, 80333 Munich, Germany

ARTICLE INFO

Article history:
Received 17 July 2014
Received in revised form
25 July 2014
Accepted 26 July 2014
Available online 1 August 2014

Keywords:
$MnWO_4$
In-doping
Defects
Rietveld analysis
X-ray powder diffraction
Micro-Raman spectroscopy

ABSTRACT

Substitution of In^{3+} for Mn^{2+} in $MnWO_4$, which is one of the most studied multiferroics, was conducted systematically by solid-state reactions at 1050 °C to obtain a series of $Mn_{(1-3x)}In_{2x}\square_xWO_4$ solid solutions ($x=0$–0.11; the box indicates vacancy). The successful In-doping could be proven by electron microprobe, and statically disordered structures of this solid solution series were elucidated by Rietveld analyses with X-Ray powder diffraction (XPD) data. Its average structure maintains the space group ***P***2/*c* at least up to the replacement of 33 at% Mn. The tendency of their unit cells proportionally enlarging with In-doping is an unexpected observation because In^{3+} is smaller than Mn^{2+}. This could not be explained alone by average atomic bonding distances and angles evaluated from XPD data analyses. Complimentarily, micro-Raman spectra of $Mn_{(1-3x)}In_{2x}\square_xWO_4$ materials feature a hardening of Raman modes due to stronger atomic bonds in W_2O_4 and WO_2 units with increasing In-doping. This is considered as an inevitable consequence of broken bonding in directly neighbouring Mn–O bonds as the presence of In^{3+} in $MnWO_4$ accompanies the creation of defects at Mn sites. The current study using XRD and micro-Raman suggests the enlarging local space around the bridging oxygen as the reason for the unexpected cell expansion when smaller In^{3+} along with defects replace Mn^{2+} in $MnWO_4$.

1. Introduction

Diverse wolframite-type AWO_4 compounds (*A*: divalent metals) have been investigated for their multifunctional properties for industrial applications, e.g. as laser crystals and phosphors [1,2]. Among them manganese tungstate ($MnWO_4$; mineral name: hubnerite [3]) is of great interest as an intensively studied multiferroic [4–8]. $MnWO_4$ undergoes three different phase transitions within a very narrow temperature range, resulting in three different antiferromagnetic phases AF3, AF2, and AF1 at 13.5 K (T_N: Neel temperature), 12.7 K (T2), and 7.6 K (T3), respectively [7]. The phase AF2 exhibits an interesting multiferroic coupling, i.e. magnetic ordering-induced electric polarization at Mn sites [7,8]. For the ease with technical application at ambient conditions it is necessary to increase the magnetic ordering transition temperatures of $MnWO_4$. In order to investigate the influence of doping on the antiferromagnetic transition in this system there were tries to investigate several solid solutions, such as $A_xMn_{1-x}WO_4$ (A=Mg, Zn, Co, Fe and Ni) [9] and $MnMo_xW_{1-x}O_4$ [5,10–13]. In all these attempts isomorphic substitution was succeeded for Mn^{2+} by divalent metals only, or W^{6+} exclusively by hexavalent Mo. This resulted in decreasing magnetic phase transition temperatures or suppressing the multiferroic state AF2 [5].

In the present study a trivalent cation, In^{3+} has been applied to obtain the solid solutions $Mn_{(1-3x)}In_{2x}\square_xWO_4$ ($\square$=vacancy, $x=0$–0.11). The creation of vacancies at Mn sites by partial replacement of In^{3+} for Mn^{2+} was aimed to introduce polar characters at Mn sites, or at least to change the local configuration between alternating Mn- and W-sheets (Fig. 1). Based on analyses of In-doped $MnWO_4$-type materials using X-ray powder diffraction (XPD) and micro-Raman spectroscopy (μ-RS), this report describes the resulting local structural changes in connection with the unexpected overall cell expansion with smaller In^{3+} for larger Mn^{2+} [14].

2. Experimental

2.1. Synthesis

Powder samples of In-doped $MnWO_4$ (In:$MnWO_4$) were synthesized via solid-state reactions in the system MnO–WO_3–In_2O_3. MnO

* Corresponding author. Tel.: +49 89 2180 4333; fax: +49 89 2180 4334.
E-mail address: sohyun.park@lmu.de (S.-H. Park).

http://dx.doi.org/10.1016/j.jssc.2014.07.039
0022-4596/

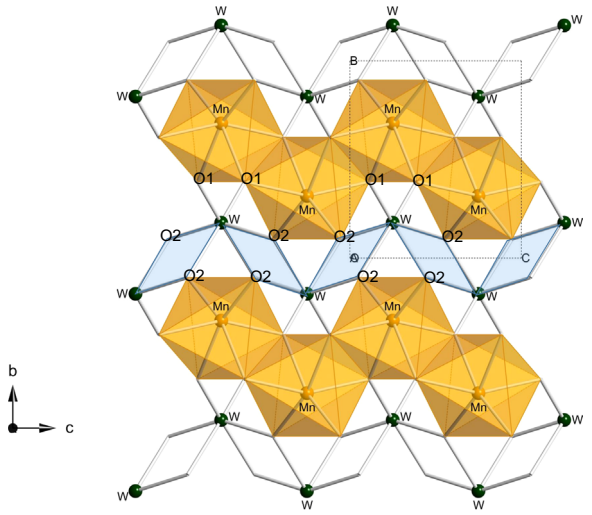

Fig. 1. Arrangement of edge-sharing chains of MnO_6 and WO_6 building units in $MnWO_4$ [3] perpendicular to the crystallographic *a*-axis. Over the bridging oxygen at the site O2 all W atoms are connected to each other to configure chains of (W_2O2_2), as highlighted.

Table 1
Synthesis conditions and products from solid-state reactions at 1050 °C. The phase identification was made based on XPD data.

Lab code	Molar ratio			Heating time [h]	Synthesis products
	Mn	In	W		
In0	1	0	1	80+60	$MnWO_4$
In5	0.95	0.05	1	60	In:$MnWO_4$, In_6WO_{12}
In7	0.90	0.07	1	12+12+12	In:$MnWO_4$
In10-1	0.90	0.10	1	80	In:$MnWO_4$, Mn_2O_3, Mn_3O_4, In_2O_3
In10-2	0.90	0.10	1	80+80	In:$MnWO_4$, In_6WO_{12}
In13	0.80	0.13	1	12+12+12	In:$MnWO_4$
In15	0.85	0.15	1	30+60+30	In:$MnWO_4$, In_6WO_{12}
In20-1	0.80	0.20	1	30+60+30	In:$MnWO_4$, In_6WO_{12}
In20-2	0.70	0.20	1	12+12+12	In:$MnWO_4$
In27	0.60	0.27	1	12+12+12	In:$MnWO_4$, $In_2W_3O_{12}$

(Alfa Aesar, 99%), WO_3 (Fluka, 99.9%), and In_2O_3 (Alfa Aesar, 99.9%) were used as starting materials without further purification. Phase purity of reactants was verified by XPD. The molar ratios of Mn:In:W in the educts were varied from 1:0:1 to 0.60:0.27:1 (Table 1). The starting oxide mixtures were ground in an agate mortar and then pressed in pellets with 80 bar using a hydraulic press. Each pellet was put into a sintered aluminium oxide crucible to allow solid-state reaction at 1050 °C in air for 12 h. After cooling fast down to 20 °C within the oven the synthesis product was characterized by XPD to check the quality of yield. The heating programme was repeated maximal three times to ensure finishing reactions completely and homogeneously (Table 1).

2.2. Chemical analysis

Chemical contents of Mn, In, and W in the selected samples (Table 2) were determined by electron microprobe (Cameca SX100) with a beam current of 40 nA at 15 kV. For performing electron microprobe powder samples were embedded in resin and then carbon coated to allow electric conductivity. InSb, metallic tungsten, and Mn-rich Ilmenite (3.69 wt% Mn, 36.17 wt% Fe, 27.40 wt% Ti, 0.64 wt% Nb, 0.19 wt% Na, 31.30 wt% O) were used as the respective reference for In, W, and Mn.

Table 2
Results from electron microprobe measurements with nine solid-solution samples given by lab codes.

Lab code	Atomic ratios		Ideal unit cell content[a]
	Mn	In	
In0	1.000(1)	0.000(1)	$MnWO_4$
In5	0.94(1)	0.04(1)	$Mn_{0.94(1)}In_{0.04(1)}{}^{\square}{}_{0.02}WO_4$
In7	0.91(2)	0.06(1)	$Mn_{0.91(2)}In_{0.06(1)}{}^{\square}{}_{0.03}WO_4$
In10-2	0.92(2)	0.05(1)	$Mn_{0.92(2)}In_{0.05(1)}{}^{\square}{}_{0.03}WO_4$
In13	0.80(2)	0.14(1)	$Mn_{0.80(2)}In_{0.14(1)}{}^{\square}{}_{0.06}WO_4$
In15	0.85(2)	0.10(2)	$Mn_{0.85(2)}In_{0.10(2)}{}^{\square}{}_{0.05}WO_4$
In20-1	0.79(2)	0.14(2)	$Mn_{0.79(2)}In_{0.14(2)}{}^{\square}{}_{0.07}WO_4$
In20-2	0.71(2)	0.19(1)	$Mn_{0.71(2)}In_{0.19(1)}{}^{\square}{}_{0.10}WO_4$
In27	0.67(1)	0.22(1)	$Mn_{0.67(1)}In_{0.22(1)}{}^{\square}{}_{0.11}WO_4$

[a] Based on one WO_4 in the unit.

2.3. X-ray powder diffraction

XPD data were collected on a X-ray powder diffractometer, *Stadi P* (STOE) using Mo$K\alpha_1$ (λ=0.7093 Å aligned with Ge(1 1 1) monochromator) at 30 mA and 50 kV in the Debye–Scherrer geometry. For conducting XPD each as-synthesized sample was grounded with Si powder as internal standard. A tiny amount of this powder mixture was deposited onto thin cellulose foil spanned between two brass rings and fixed with glue (*Celit*). Data collection was made while rotating the sample holder for better counting statistics. For each data set the reciprocal space range of 5–65°(2θ) was recorded on a 5° (2θ)-linear position-sensitive detector in every 0.1°(2θ) for 20 s., resulting in a step size of 0.02°(2θ). Each XPD pattern was recorded six times, and they were added up to increase the signal-to-noise ratio. Phase identification with XPD data was made based on the data bank *inorganic crystal structure database* (*ICSD*) [15] with the interface *FindIt* [15] to provide starting models for structure refinements. Rietveld calculations were performed using the programme package *FullProf Suite* [16].

2.4. Micro-Raman spectroscopy

μ-RS of as-synthesized samples were acquired from 100 to 1200 cm^{-1} on a micro-Raman spectrometer (*HORIBA*; *XploRa-Raman-System*) using red laser (638 nm) at 9.30 mW.

For comparison Raman spectra with hubnerite crystallites were measured. This sample registered with the ID: 200334 was kindly provided by Mineralogische Staatssammlung München. The Raman system *Olympus* was set with 100% filter, 1200T grating, and a 100 × long-wide distance objective. The beam was transmitted to the spectrometer through an optical fibre with a 50 μm diameter core as pinhole, giving a beam diameter of 0.7 μm on the sample surface. The diffraction limited focus had a lateral resolution of 400 nm and a focal depth of 800 nm. The power distribution of the beam profile was Gaussian. Elastically scattered photons were suppressed via a sharp edge filter, and the instrument calibration was done with a silicon standard. Acquired Raman spectra were further analysed using a curve fitting and data processing software, FITYK [17]. A linear baseline subtraction, a 5% smoothing with fast Fourier transform, and a Gaussian–Lorentzian function were applied for convoluting Raman spectral profiles.

3. Results and discussion

3.1. Synthesis products

Crystalline products from solid-state reactions are listed in Table 1. They are named by **In#**, where **#** indicates the number